Biphasic oxidation reactions promoted by amphiphilic catalysts based on red mud residue

A.A.S. Oliveira [a], I.F. Teixeira [a], Taís Christofani [a], J.C. Tristão [b], I.R. Guimarães [c], F.C.C. Moura [a],*

[a] Departamento de Química, ICEx, Universidade Federal de Minas Gerais, Av. Antônio Carlos, 6627, Pampulha, Belo Horizonte/MG, CEP 31270-901, Brazil
[b] Departamento de Química, Universidade Federal de Viçosa, Rodovia LMG 818, km 06, Florestal/MG, CEP 35690-000, Brazil
[c] Departamento de Química, Universidade Federal de Lavras, Campus Universitário, Caixa Postal 3037, Lavras/MG, CEP 37200-000, Brazil

ARTICLE INFO

ABSTRACT

Biphasic oxidation reactions of organic contaminants with H_2O_2 were promoted by amphiphilic catalysts prepared from red mud residue and carbon nanostructures. Contaminants oxidation is especially important for petroleum treatment, since S and N compounds are extremely unwanted mainly due to environmental issues. Also, government regulations around the levels of these pollutants in fuels are becoming increasingly strict. The amphiphilic catalysts were tested in oxidation of different model molecules: Sudan IV lipophilic dye, tiophene, dibenzothiophene and quinoline and showed very good removal, reaching 100% of contaminants oxidation. The amphiphilic catalysts act in two steps of biphasic oxidation: (i) favor the formation of a reversible emulsion between the organic contaminated phase and the aqueous oxidized phase and (ii) catalyze Fenton reaction. After reaction, the emulsion can be easily separated by a magnetic process into two phases: decontaminated organic phase and aqueous phase with oxidized contaminants.

© 2013 Elsevier B.V. All rights reserved.

1. Introduction

Red mud (RM) is a by-product of aluminum extraction from bauxite ores via the Bayer process [1]. It is estimated that for each ton of alumina (Al_2O_3) produced, 0.5–2 tons (on a dry weight basis) of red mud is generated with a global production of about 120 million tons of red mud per year [1–3]. RM exhibits several environmental hazards due to its high alkalinity (pH > 11), sodium and heavy metal contents [3] and in some cases, large volumes stored in inappropriate areas. In 2010, a red mud reservoir in Hungary collapsed and ca. $700.000 m^3$ of the mud with a pH around 12 was released from the reservoir to the nearby cities [4] causing 12 deaths and lots of injury.

In this context, the development of technologies to give red mud a proper destination is of great interest. RM has been applied in different areas, such as metallurgy (recovery of metals [5]), wastewater and waste gas treatment [6], sorption of contaminants [7–9], agriculture, building construction and ceramics [10]. RM has also been used in catalytic applications [11]. Some of these uses as catalysts are in hydrogenations (e.g. of toluene [12], tetrachloroethylene [13,14] and polyaromatic compounds such as

anthracene oil [15,16], naphthalene [17], phenanthrene and pyrene [18]), in oxidations (e.g. of methane [19], chlorohydrocarbons [20], plastic wastes [21] and other volatile organic compounds (VOCs) [22,23]), in catalytic pyrolysis of plastic wastes [24], in upgrading of pyrolysis bio-oil [25], and also as support for catalytic ammonia decomposition [26].

Nowadays there is also an increasing environmental concern about the pollution caused by fossil fuels. During fuel combustion, molecules containing S or N form SO_x and NO_x pollutants, the main responsible for acid rain. Moreover, S-contaminants poison car catalysts preventing them to remove most of the gas pollutants produced during combustion. Ever stricter legislation has been implemented all over the world to limit the content of sulfur and nitrogen in petroleum fuels. And for this reason, the development of new technologies for S and N removal are necessary.

In this work, biphasic oxidations promoted by modified red mud were studied. Red mud was modified by controlled CVD [27] to produce amphiphilic catalysts that act on the interface of biphasic systems [28], especially for oxidation reactions.

Chemical vapor deposition (CVD) is currently the most common technique to grow carbon nanostructures, such as CNTs [29]. Several reasons explain this preference. First, it is technically easy to carry out as in its simplest version it only requires an oven, a tubular reactor, and a set of mass flow controllers to feed the gas mixture. Secondly, a large number of parameters can still be varied
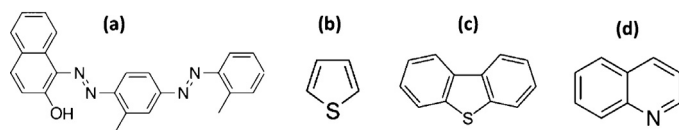

Fig. 1. Chemical structure of substances used in oxidation tests: (a) Sudan IV dye, (b) tiophene, (c) dibenzothiophene and (d) quinoline.

and investigated, both during the catalyst treatment and the CNT growth, which influence both the yield and quality of the CNTs [30].

The mechanism more accepted nowadays for the growth of carbon nanofilaments is known as the vapor–liquid–solid (VLS) mechanism. The VLS mechanism comprises three successive steps. Firstly, a carbon containing gas precursor adsorbs and dissociates on the surface of the catalyst particle to form elementary carbon atoms. Secondly, the carbon atoms dissolve in the bulk of the nanoparticles to form a liquid metastable carbide and diffuse within the particle. Finally, solid carbon precipitates at the rear side of the nanoparticles to form a carbon nanofilament [30].

The reproducibility of CVD synthesis is shown by several works [31,32]. In the last five years, CNTs have been produced in large scale by CVD technique. Nowadays, the parameters to control the characteristics and reproducibility of CNT synthesis are well known.

Recent studies have shown that amphiphilic materials are very efficient in biphasic reactions [33–35], because of their ability to form emulsions between immiscible liquids [28].

Hereon, it is described the application of magnetic amphiphilic composites produced from red mud to promote biphasic oxidation with H_2O_2 of four hydrophobic molecules: Sudan IV dye, thiofene and dibenzothiofene (models for sulfur containing contaminants of petroleum industry) and quinoline (model for nitrogen containing contaminant of petroleum industry). These materials also have the ability of breaking emulsions under action of an external magnetic field, enabling the easy separation of the phases and recovering of the catalyst.

2. Experimental

For the production of amphiphilic catalysts CVD (chemical vapor deposition) reactions were carried out with ethanol at ca. 6% in N_2 and 50 mg of red mud. The reaction was quenched at 700, 800 and 900 °C and the catalysts were named as RmEt700, RmEt800 and RmEt900, respectively. These catalysts produced were extensive characterized [27].

In order to evaluate the interaction of the catalysts on the interface of biphasic systems they were tested as emulsifiers and demulsifiers. Mixtures of water/cyclohexane were used to simulate petroleum mixtures with water. These mixtures were emulsified via addition of the amphiphilic catalysts (500 mg L^{-1}) and sonication. Stable emulsions were formed and characterized by optic

microscopy (Cole Parmer Instrument, 41500-50). These emulsions are naturally broken (phases separated) within 24 h. However, if an external magnetic field is approximated to the emulsion, it can be separated in 2 min.

Due to their amphiphilic properties the catalysts were employed in heterogeneous Fenton reactions in biphasic systems. Oxidation reactions were carried out with 5 mL of organic phase (500 mg L^{-1} in cyclohexane), 1 mL of aqueous phase of hydrogen peroxide (H_2O_2 30%) and 20 mg of the catalyst. The catalysts were left previously in contact only with the organic phase until adsorption equilibrium was reached. Sudan IV (Fig. 1(a)) removal was monitored by UV/vis spectroscopy (Shimadzu UV-2550 – characteristic wavelength 510 nm) and thiophene (Fig. 1(b)) removal by gas chromatography with FID detector (GC/FID, Shimadzu GC17A). Dibenzothiophene (Fig. 1(c)) and quinoline (Fig. 1(d)) oxidations were monitored by gas chromatography coupled to mass spectroscopy (GC/MS, Shimadzu QP2010 – PLUS). Oxidized products extracted by aqueous solution were analyzed by electrospray ionization mass spectrometry (ESI/MS, Agilent ion trap mass spectrometer). Reduction of contaminants concentration was studied over time.

Reuse tests of the amphiphilic catalysts were carried out. The catalysts were used up to five times with fresh solutions of oxidant and contaminants. Metal leaching was also measured after experiments by atomic absorption spectrometry.

3. Results and discussion

Pure red mud was characterized by atomic absorption spectrometry, energy dispersive spectroscopy (EDS), Mössbauer spectroscopy, X-ray diffraction and Raman Spectroscopy. The results showed the presence of 20 wt% of Fe (as Fe_2O_3) and Al_2O_3 (22%), CaO (5%), Na_2O (6%), MnO (0.4%), SiO_2 (11%), TiO_2 (3%) as the main components.

CVD reaction of ethanol and red mud (RM) was studied by TPRe (Temperature Programmed Reaction) experiments. It was observed that during CVD process ethanol reacts with RM promoting the reduction of the iron phase with carbon formation. The resulting composites based on reduced iron phases and carbon deposited on the surface were characterized by Mössbauer spectroscopy, XRD, CHN, BET surface area, SEM, TEM and Raman spectroscopy. The results showed a complex structure with magnetic and amphiphilic properties [27] as depicted in Fig. 2.

The magnetic property of the catalysts is a consequence of reduction of the iron phases present in RM to metallic iron Fe^0 and iron carbide Fe_3C. The distribution of these reduced iron phases vary with CVD temperature but all the catalysts produced are magnetic. Iron phases distribution was determined by Mössbauer spectroscopy. Table 1 shows the Mössbauer hyperfine parameters used for phase determination and also the relative subspectral area of each iron phase.
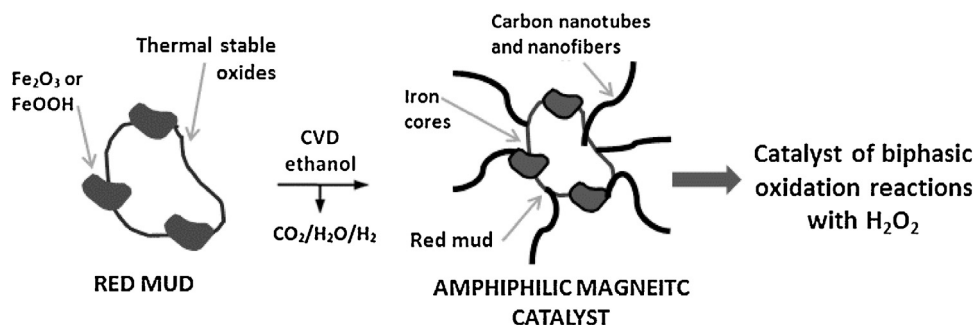

Fig. 2. Schematic structure of the composites obtained after CVD reaction of red mud with ethanol.
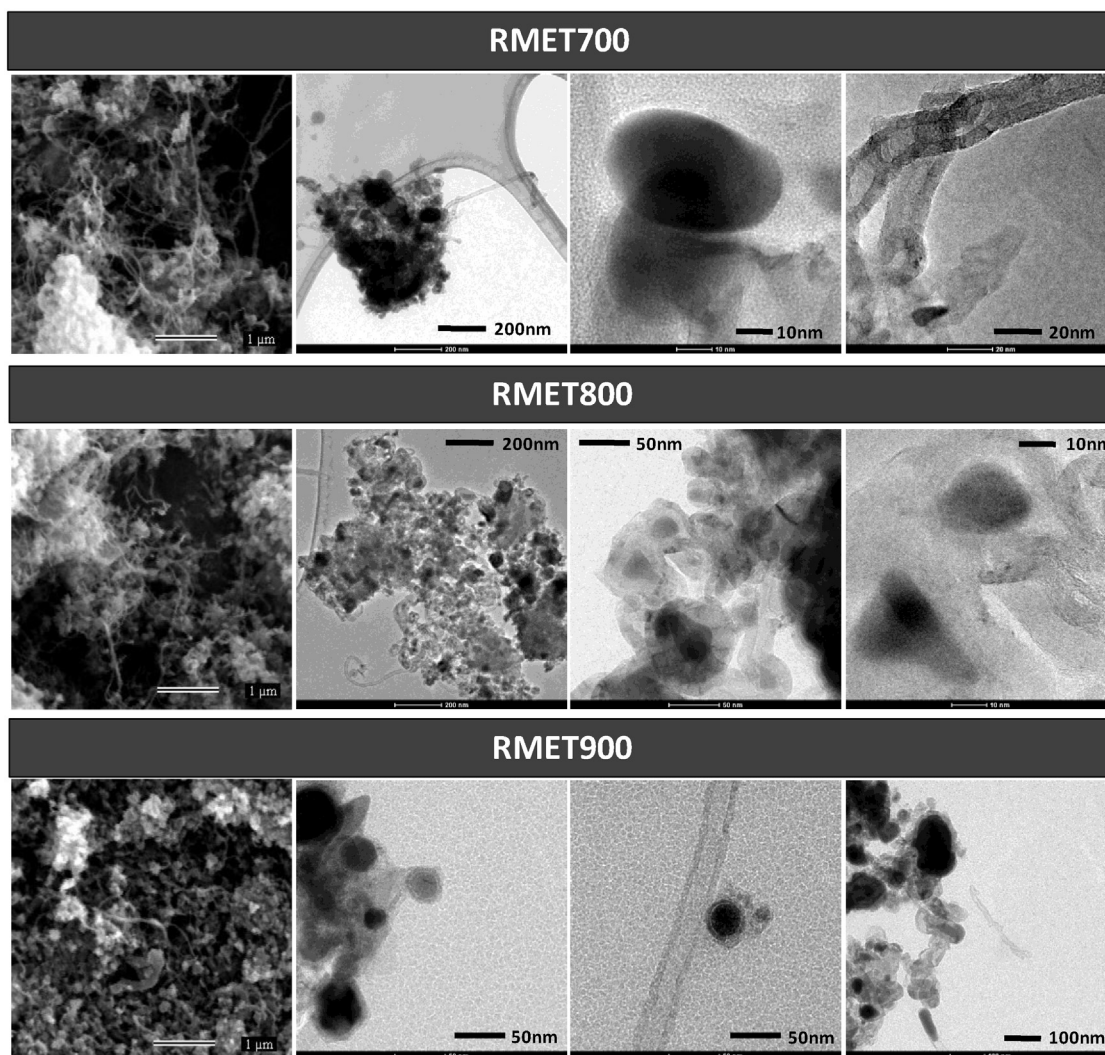
Fig. 3. SEM and TEM images of red mud catalysts.

It is possible to observe in Table 1 that hematite (α-Fe_2O_3) is present only in RM composition. After CVD with ethanol at 700, 800 or 900 °C hematite is reduced to Fe^0 and Fe_3C, magnetic iron phases.

The amphiphilic property of RM catalysts is a result of the combination of thermally stable oxides of RM (e.g. SiO_2, Al_2O_3 and TiO_2), which are hydrophilic, with a partial coverage of hydrophobic carbon nanostructures, such as carbon filaments. Surface area of the catalyst varies from 67 to 79 $m^2\,g^{-1}$ while RM presents surface area of 24 $m^2\,g^{-1}$, obtained by N_2 adsorption. Carbon content of the catalysts is 27, 30 and 42% for RmEt700, 800 and 900, respectively (CHN results). Carbon is distributed mainly as well organized forms (graphitic structures) shown by Raman spectroscopy in Supplementary Material. Raman spectra obtained show intense G band (related to organized carbon) and RBM bands that suggest the presence of single wall carbon nanotubes [27]. SEM and TEM images

Table 1
Hyperfine parameters determined for RM and catalysts produced by CVD with ethanol.

Sample	Site/phase	δ/mm s^{-1} (0.05)	ε, Δ/mm s^{-1} (0.05)	B_{hf}/T (0.05)	Relative subspectral area/%
RM	α-Fe_2O_3	0.36	−0.21	51.4	52
	Fe^{3+}	0.36	0.58	–	48
RmEt700	Fe^0	0.00	0.00	33.00	22
	Fe_3C	0.17	0.03	20.60	48
	Fe^{3+}	0.40	0.80	–	30
RmEt800	Fe^0	0.00	0.00	33.00	25
	Fe_3C	0.18	0.01	20.6	59
	Fe^{3+}	0.25	0.8	–	16
RmEt900	Fe^0	0.00	0.00	33.00	18
	Fe_3C	0.18	0.03	20.8	65
	Fe^{3+}	0.18	0.70	–	17

δ – Isomeric shift relative to α-Fe; ε – quadrupole shift; Δ – quadrupole splitting; B_{hf} – hyperfine magnetic field.

Fig. 4. Images of contact angle between catalysts and water droplet.

(Fig. 3) show irregular carbon filaments which are likely responsible for the increase on the surface area of the composites (from $24\,m^2\,g^{-1}$ of RM to ca. $80\,m^2\,g^{-1}$). The surface area of RM and catalysts was determined by N_2 adsorption and the BET method. Pure red mud presents a surface area of $24\,m^2\,g^{-1}$ and RmEt700, 800 and 900 show areas of 79, 68 and $67\,m^2\,g^{-1}$, respectively. More than that, pores distribution were studied by the BET method and it shows important differences between pure RM and catalysts. Red mud presents the majority of its pores with diameters greater than 100 nm, in the region of macro pores, which explains its low value of surface area. On the other hand, RmEt700 catalyst presents mesopores smaller than 10 nm, providing an increase in the surface area (24–$79\,m^2\,g^{-1}$). In RmEt800 and 900 catalysts, which showed intermediate areas, mesopores smaller than 10 nm are still observed, but in less quantity, and macropores are in greater proportion than in RmEt700 (Supplementary Material – Fig. S5).

In SEM and TEM images of Fig. 3 it is possible to observe nanometric Fe particles inside of the carbon filaments while large metallic aggregates appear covered with amorphous carbon. The carbon filaments are in average 20 μm long with diameters varying from 10 up to 100 nm.

As shown in Fig. 3, the catalysts comprise a hydrophilic portion composed by the oxides, e.g. SiO_2, Al_2O_3 and TiO_2, present in the red mud and a hydrophobic portion that consists of carbon nanostructures partially covering the materials surface. It is observed that RmEt700 exhibits more C filaments than RmEt800 and 900. This is likely due to a sinterization process that takes place with the increase of CVD reaction temperature.

The hydrophobicity of the composites can be tuned by the carbon content, which can improve the interaction with organic phase. Contact angle images (Fig. 4) show that RmEt900 (42% C) is a little more hydrophobic and interacts less with a water droplet than

RmEt700 (27% C). However, both catalysts are still amphiphilic, showing contact angles close to 60°.

As a result of this amphiphilic character the catalysts interact both with aqueous and organic liquids at the same time and can be used to form and break emulsions.

The efficiency of the composites to form emulsions was investigated with an immiscible mixture of cyclohexane and water. No emulsification took place with these mixtures even after 25 min under sonication. On the other hand, in the presence of $500\,mg\,L^{-1}$ of the amphiphilic composite the mixture emulsified with only 2 min sonication. Fig. 5 shows images of the heterogeneous mixture after addition of the amphiphilic materials and also the emulsified system in macro and microscopic view.

Using an optical microscope it was observed that an emulsion is formed (Fig. 5(b)) between two immiscible liquids (Fig. 5(a)) because small droplets of one phase are dispersed into the other. This system is stabilized by the amphiphilic particles which involve the surface of the droplets, interacting at the same time with the dispersed and the continuous phase. Fig. 5(d) shows microscopic images of cyclohexane/water emulsion stabilized by the amphiphilic catalysts. When the phases need to be separated, after catalytic reaction, an external magnetic field can be approximated and the emulsion is broken (Fig. 5(c)). The catalysts are then attracted and destabilize the emulsion. This destabilization is mainly mechanical. Since the particles are removed and are not involving the interface of the droplets the two immiscible liquids separate themselves, which means that the coalescence of the system takes place. The reusability of the materials was tested showing good results for at least 5 sequence tests.

The amphiphilic catalysts produced from RM were used to promote biphasic oxidation of different organic contaminants with aqueous H_2O_2. Emulsification of organic phase and aqueous phase containing the oxidant promotes an excellent contact between reactant species, strongly favoring the oxidation process. After reaction, the emulsion can be easily separated by a magnetic process into two phases: decontaminated organic phase and aqueous phase with oxidized contaminants. Fig. 6 shows a possible pathway for the improved oxidation promoted by the RM composites.

The formation of an emulsion stabilized by the amphiphilic nanoparticles produces a much more extended interface between oil phase and H_2O_2 (aq) (Fig. 6(a) and (b)). Hydrogen peroxide is then activated on the surface of amphiphilic nanoparticles due to the presence of exposed reduced iron phases by a heterogeneous
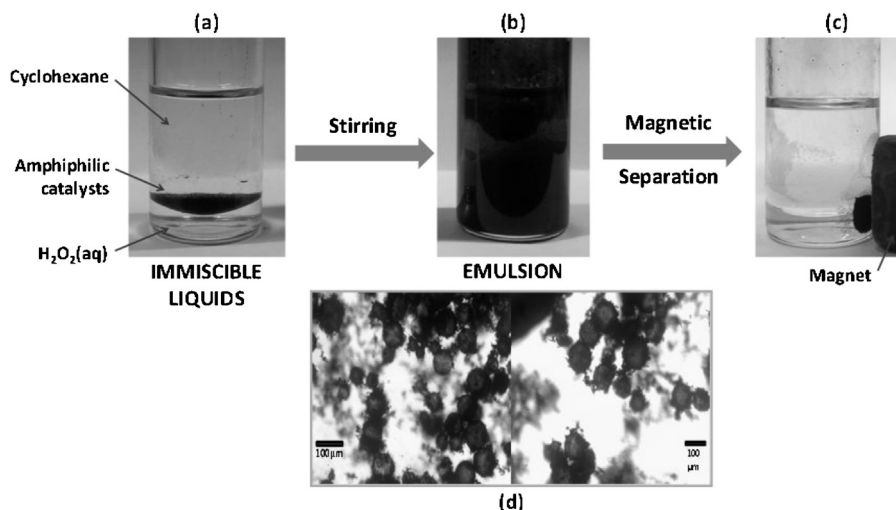

Fig. 5. Schematic images of formation and breaking of emulsions using the amphiphilic catalysts, macro and microscopic views.
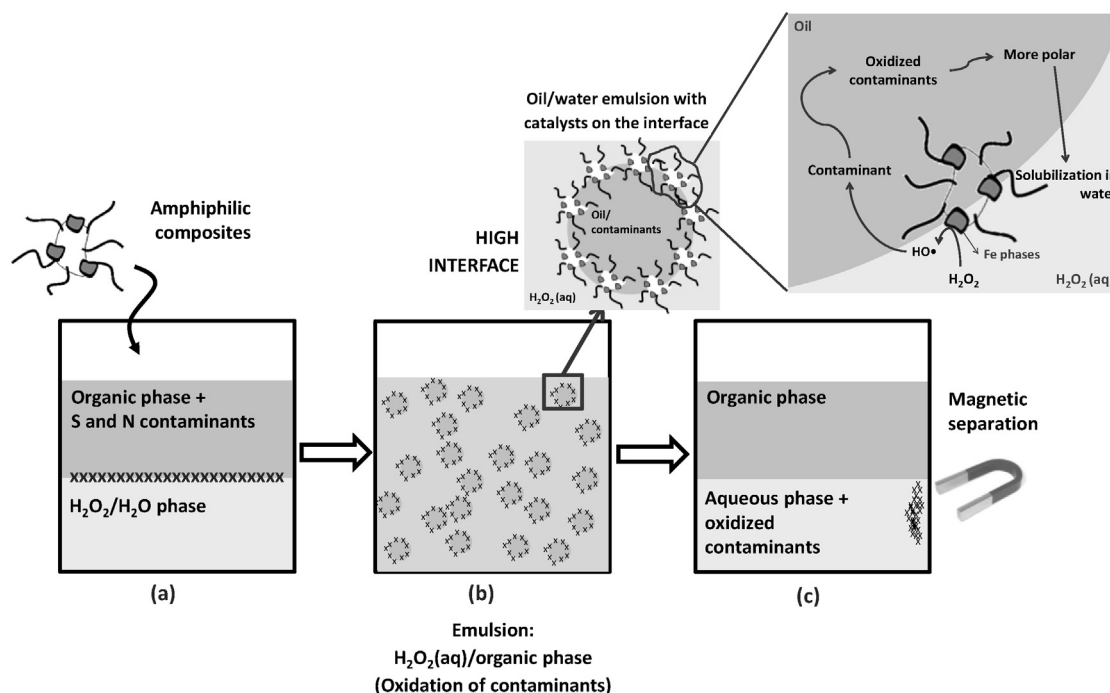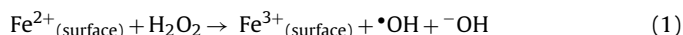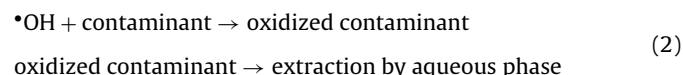
Fig. 6. Possible mechanism for biphasic oxidation reactions promoted by RM amphiphilic catalysts.

Fenton like mechanism, forming highly oxidizing hydroxyl radicals ($^\bullet$OH) on the oil/water interface (Eq. (1)).

$$Fe^{2+}_{(surface)} + H_2O_2 \rightarrow Fe^{3+}_{(surface)} + {}^\bullet OH + {}^- OH \qquad (1)$$

Consequently, $^\bullet$OH radicals can act in the oxidation of the contaminant present in organic phase. The polar oxidized contaminants diffuse to aqueous phase by polarity (Fig. 6(b) – detail) and are extracted (Eq. (2)).

$$^\bullet OH + contaminant \rightarrow oxidized\ contaminant$$
$$oxidized\ contaminant \rightarrow extraction\ by\ aqueous\ phase \qquad (2)$$

After reaction, the amphiphilic catalysts can be removed by a simple magnetic field and the emulsion is broken (Fig. 6(c)). All experiments were carried out at pH near 6–7. In some initial experiments, aqueous phase pH was monitored and no significant change under these conditions was observed.

The oxidation of four organic substrates was investigated: (i) Sudan IV lipophilic dye, (ii) thiophene, (iii) dibenzothiophene (DBT) and (iv) quinoline. The catalysts were left in contact with the substrate solutions before addition of the oxidant until they reached adsorption equilibrium. It is observed that less than 5% of contaminants tested are adsorbed on the surface of catalysts in 60 min. More than that, it is expected, based on the mechanism proposed, that even the molecules adsorbed on the surface of catalysts are oxidized in the presence of H_2O_2.

In Fig. 7 it is possible to see the results obtained for Sudan IV and thiophene oxidations.

Oxidation reactions in organic phase were held using Sudan IV dye as a model contaminant (Fig. 7(a)). Hydrogen peroxide is highly hydrosoluble, while Sudan IV is only soluble in organic solvents. The amphiphilic catalysts were used to promote the interface and also to facilitate the reaction between H_2O_2 and Sudan IV. The initial oxidation process was monitored by UV/vis spectroscopy. No reduction of the dye color was observed in the absence of the catalysts, even in the presence of pure red mud. On the other hand, the catalysts showed good efficiency in the removal of Sudan IV dye from oily phase by Fenton, reaching ca. 80% of color removal in 1 h.

This result suggests that these composites can be used in similar reactions for other contaminant oxidations, such as nitrogen and sulfur compounds.

In Fig. 7(b) it is observed the thiophene removal promoted by the amphiphilic materials. A very small reduction (6%) in thiophene concentration is observed in the absence of the composites (blank experiment). However, the removal of thiophene reaches 67% in an hour in the presence of the amphiphilic composites (i.e. RmEt700). The increase of efficiency can be attributed to the formation of an emulsion between organic and aqueous phases promoted by the amphiphilic materials and to catalysis of heterogeneous Fenton reactions.

Experiments of dibenzothiophene (DBT) oxidation in biphasic system were studied with pure RM and the amphiphilic catalysts RmEt700, 800 and 900. The organic phase was analyzed in the beginning of reaction, i.e. 0 and 15 min, by GC–MS. (gas chromatography coupled to mass spectroscopy) and the aqueous phase was analyzed by electrospray ionization mass spectrometry (ESI-MS) at the end of the reaction, i.e. 60 min.

Fig. 8(a) shows DBT removal (%) by oxidation with RM catalysts in different times of reaction. Fig. 8(b) shows chromatograms obtained by GC–MS. within 15 min of reaction showing the formation of the oxidized product.

Without catalyst no removal of DBT can be observed within 1 h. Experiments with pure RM showed ca. 12% of DBT oxidation. Pure RM acts in the limited interface mainly via homogeneous Fenton due to its partial solubility in water. Moreover, the pure residue can leach other undesired metals to the solution that cannot be removed magnetically. On the other hand, the composites produced via CVD of RM with ethanol are not soluble and exhibit good efficiency in the oxidation of DBT. Efficiencies vary from 70 up to 82% in 60 min for RmEt700 and 800, respectively (Fig. 8(a)). This result suggests that DBT oxidation depends on the characteristics of the catalyst, e.g. hydrophobicity level, since RmEt800 seems to have the best combination of amphiphilicity and iron availability for Fenton reaction. It is observed that longer times of reaction, i.e. 3 h and 12 h, do not influence significantly on the oxidation percentage.
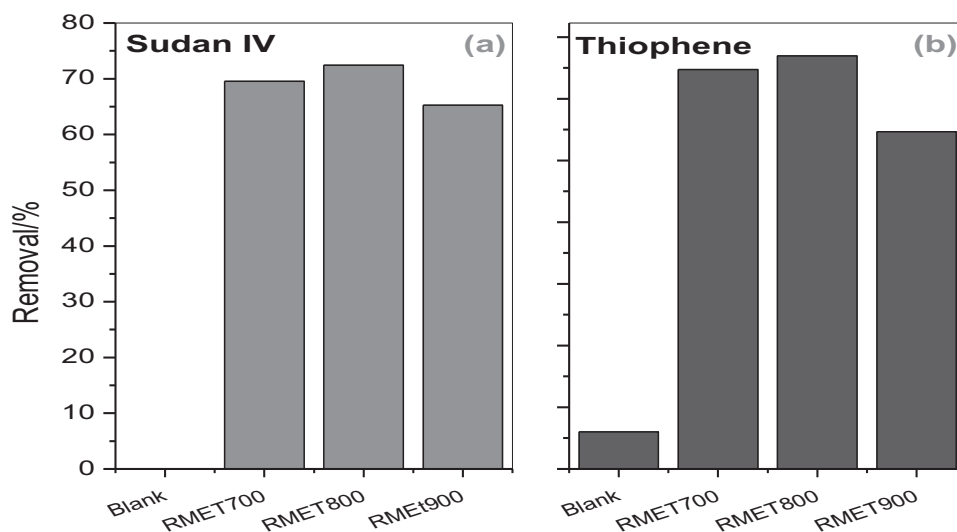
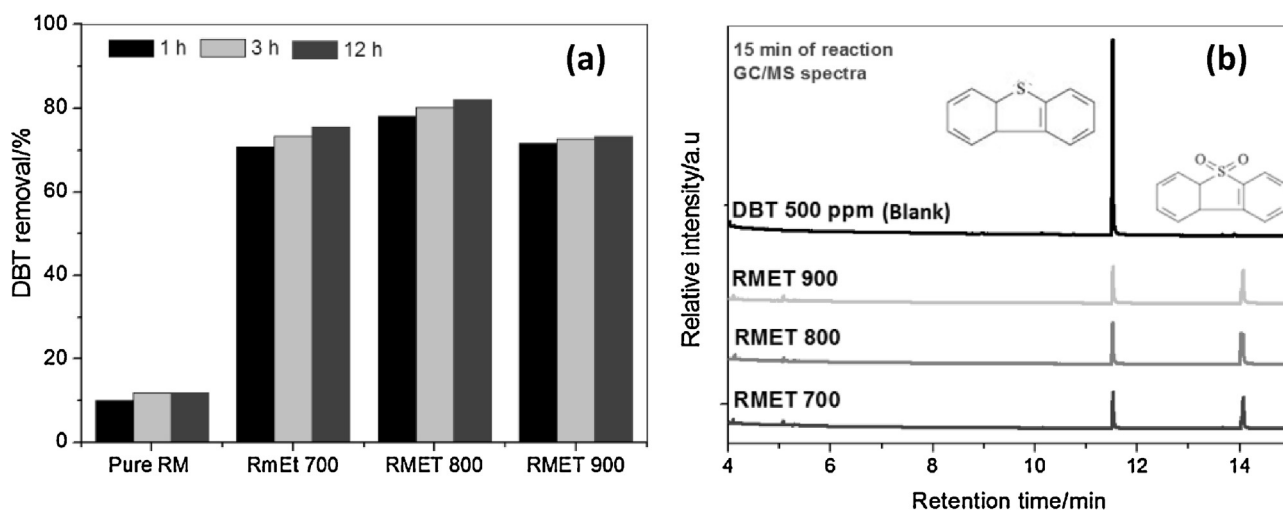**Fig. 7.** Removal of Sudan IV and thiophene by catalytic oxidation reactions.

Fig. 8. Monitoring of (a) DBT and (b) oxidized product DBTO$_2$ in organic phase by GC–MS.

The gas phase of the reaction was analyzed in order to observe if DBT oxidation could lead to gas products formation. However, no gas products containing S were identified, suggesting that all oxidation products remain in organic phase or are transferred to aqueous phase.

By GC–MS it was observed that the concentration of oxidized species in organic phase increases in the first minutes of reaction in the presence of the amphiphilic catalysts (0–15 min – Fig. 8(b)). However, the signal referent to the oxidized species (i.e. sulfone) decreases after 15 min, suggesting that this polar molecule is extracted by the aqueous phase. These observations are in agreement with the mechanism proposed in Fig. 6. The main oxidized product formed by DBT (m/z 184) oxidation is dibenzothiophene sulfone (DBTO$_2$ – m/z 216) determined by GC–MS.

Monitoring of species in aqueous phase was also carried out by ESI-MS (Fig. 9). In the beginning of reaction ($t = 0$ min) no signal is observed in the ESI-MS spectrum.

At the end of reaction ($t = 60$ min), an intense signal of m/z ratio 216 can be seen in the spectrum obtained of the aqueous phase. This signal is referent to dibenzothiophene sulfone, the same oxidized product identified in the first minutes of reaction in organic phase by GC–MS. This result confirms that DBT is oxidized and the more polar oxidized specie is extracted by aqueous phase.

The nitrogen model contaminant of petroleum and its derivatives, quinoline, was also oxidized by H$_2$O$_2$ in presence of the amphiphilic composites (Fig. 10).

The obtained results showed that the amphiphilic materials promote ca. 90% of quinoline oxidation by H$_2$O$_2$ within 30 min of reaction. Within 60 min RmEt800 catalyst reached 100% of quinoline oxidation. Without the amphiphilic catalyst only 10% of the contaminant was removed from organic phase.
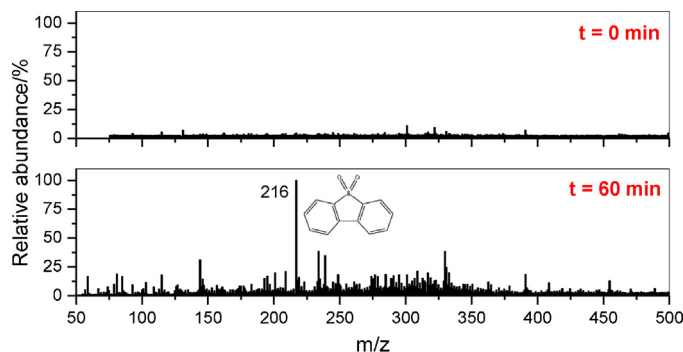

Fig. 9. Monitoring of DBT species in aqueous phase by ESI-MS.
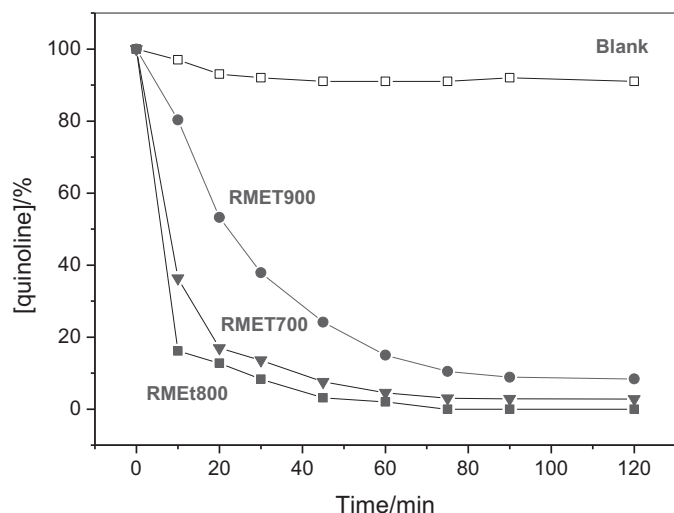
Fig. 10. Removal of quinoline by oxidation reactions catalyzed by RM composites.

Unlike the reaction with DBT, the oxidized intermediates of quinoline are not stable in organic phase, so they could not be identified by GC–MS. In a short time they can already be seen in aqueous phase by ESI-MS, especially m/z 162, corresponding to quinoline + 2OH. Fig. 11 shows ESI-MS spectra obtained after 0 and 60 min of reaction.

Quinoline is slightly soluble in aqueous phase and since no other component of this phase is identified by ESI-MS, its signal represents 100% of relative abundance in the beginning of reaction. Within 60 min a product with m/z 162 is formed in greater concentration than quinoline in aqueous phase. This product was characterized as quinoline + 2OH, formed during the oxidation process in the presence of the amphiphilic catalysts. Gas products containing N were not identified during quinoline oxidation reactions.

The mechanism of quinoline and DBT oxidation depends on two processes. Firstly the hydrogen peroxide is activated by heterogeneous fenton [36], this step is performed by exposed reduced iron phases [37], producing •OH radicals. These radicals are the responsible for the quinoline and DBT oxidation, the intermediate species of this reaction are well known Fig. S9 [38,39] and Fig. S10 [40].

In general, it is possible to say that the amphiphilic catalyst produced from RM and ethanol at 800 °C exhibits slightly higher

activity for all oxidations studied. This is likely related to the amount and distribution of carbon deposits, which interfere on the amphiphilicity and iron availability of the catalysts.

Reuse tests of the amphiphilic catalysts were carried out. The catalysts were used up to 5 times with fresh solutions of oxidant and contaminants. Their efficiency was kept approximately constant during the cycles of reuse. After 5 sequence reactions the catalysts may also be reactivated by heating under inert atmosphere.

Metals leaching were also measured after experiments by atomic absorption spectrometry. Results showed that no more than 1% of the iron contained in the materials leach during the experiment. Moreover, the leachate was tested for homogeneous Fenton and no removal of DBT or quinoline oxidation was observed.

4. Conclusion

The results obtained in this work showed that red mud, a worthless residue, can be transformed in very attractive and active catalysts by a simple and low cost process, reducing environmental impact. These catalysts are especially interesting for reactions in biphasic systems, such as oxidation of organic compounds with H_2O_2.

The catalysts have proved to be effective in all stages of a biphasic oxidation process: (i) emulsification between organic and aqueous phases, (ii) oxidation of different contaminants, i.e. Sudan IV dye, thiophene, dibenzothiophene or quinoline, and (iii) separation of the phases after reaction with extraction of oxidized contaminants. The use of biphasic systems shows the advantage to remove the oxidized products by extraction to the aqueous phase, as proven by ESI-MS.

Further experiments are being carried out to better investigate the oxidation promoted by the amphiphilic composites, especially using a real fuel and also other applications for the catalysts.

Appendix A. Supplementary data

Supplementary data associated with this article can be found, in the online version, at http://dx.doi.org/10.1016/j.apcatb.2013.07.015.
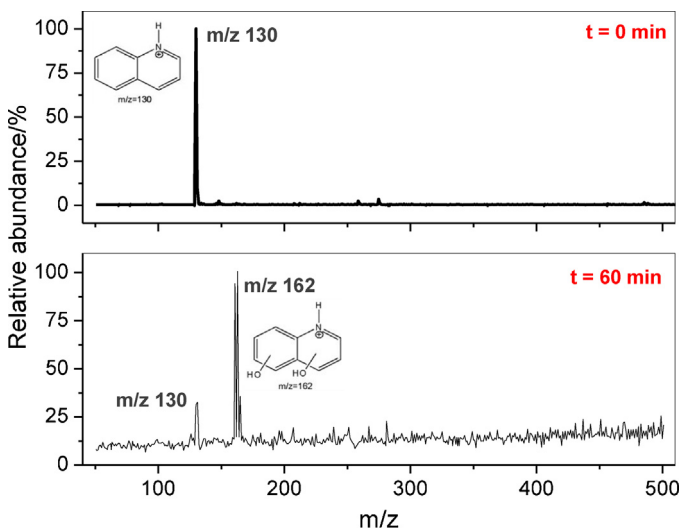

Fig. 11. Monitoring of quinoline species in aqueous phase by ESI-MS.

References

[1] S. Kumar, R. Kumar, A. Bandopadhyay, Resources Conservation and Recycling 48 (2006) 301–314.
[2] Brazilian Mineral Data Base, Departamento Nacional de Produção Mineral, 2010.
[3] J. Rivas Mercury, A.A. Cabral, A.E.M. Paiva, R.S. Angelica, R.F. Neves, T. Scheller, Journal of Thermal Analysis and Calorimetry 104 (2011) 635–643.
[4] A. Gelencser, N. Kovats, B. Turoczi, A. Rostasi, A. Hoffer, K. Imre, I. Nyiro-Kosa, D. Csakberenyi-Malasics, A. Toth, A. Czitrovszky, A. Nagy, S. Nagy, A. Acs, A. Kovacs, A. Ferincz, Z. Hartyani, M. Posfai, Environmental Science & Technology 45 (2011) 1608–1615.
[5] W.C. Liu, J.K. Yang, B. Xiao, Journal of Hazardous Materials 161 (2009) 474–478.
[6] M. Goncalves, L.C.A. Oliveira, M.C. Guerreiro, Quimica Nova 31 (2008) 518–522.
[7] S.H. Lin, R.S. Juang, Journal of Environmental Management 90 (2009) 1336–1349.
[8] E.B. da Silva, M.C.M. Alves, M. da Motta, E.H.D. Oliveira, W.B. Junior, Quimica Nova 31 (2008) 985–989.
[9] A.A.S.J.C. Tristão, J.D. Ardisson, R.M. Lago, Hyperfine Interactions 195 (2009) 21–25.
[10] Y. Pontikes, G.N. Angelopoulos, Advances in Applied Ceramics 108 (2009) 50–56.
[11] C. Klauber, M. Grafe, G. Power, Hydrometallurgy 108 (2011) 11–32.
[12] K. Pirkanniemi, M. Sillanpaa, Chemosphere 48 (2002) 1047–1060.
[13] S. Ordonez, F.V. Diez, H. Sastre, Catalysis Today 73 (2002) 325–331.

[14] S. Ordonez, H. Sastre, F.V. Diez, Journal of Hazardous Materials 81 (2001) 103–114.

[15] J. Alvarez, S. Ordonez, R. Rosal, H. Sastre, F.V. Diez, Applied Catalysis A – General 180 (1999) 399–409.

[16] H. Sun, S. Wang, H.M. Ang, M.O. Tade, Q. Li, Chemical Engineering Journal 162 (2010) 437–447.

[17] K.C. Pratt, V. Christoverson, Fuel 61 (1982) 460–462.

[18] A. Eamsiri, W.R. Jackson, K.C. Pratt, V. Christov, M. Marshall, Fuel 71 (1992) 449–453.

[19] J.R. Paredes, S. Ordonez, A. Vega, F.V. Diez, Applied Catalysis B – Environmental 47 (2004) 37–45.

[20] J. Halasz, M. Hodos, I. Hannus, G. Tasi, I. Kiricsi, Colloids Surfaces A – Physicochemical and Engineering Aspects 265 (2005) 171–177.

[21] J. Yanik, M.A. Uddin, K. Ikeuchi, Y. Sakata, Polymer Degradation and Stability 73 (2001) 335–346.

[22] J.F. Lamonier, F. Wyralski, G. Leclercq, A. Aboukais, Canadian Journal of Chemical Engineering 83 (2005) 737–741.

[23] M. Hoang, Pct Int. Pat. WO 00/00285 Ref. CAS 132:68653, 2000.

[24] A. Lopez-Urionabarrenechea, I. de Marco, B.M. Caballero, M.F. Laresgoiti, A. Adrados, A. Aranzabal, Applied Catalysis B – Environmental 104 (2011) 211–219.

[25] E. Karimi, I.F. Teixeira, L.P. Ribeiro, A. Gomez, R.M. Lago, G. Penner, S.W. Kycia, M. Schlaf, Catalysis Today, 2012, 73-88.

[26] P.F. Ng, L. Li, S.B. Wang, Z.H. Zhu, G.Q. Lu, Z.F. Yan, Environmental Science & Technology 41 (2007) 3758–3762.

[27] A.A.S. Oliveira, J.C. Tristao, J.D. Ardisson, A. Dias, R.M. Lago, Applied Catalysis B 105 (2011) 163–170.

[28] A.A.S. Oliveira, I.F. Teixeira, L.P. Ribeiro, J.C. Tristao, A. Dias, R.M. Lago, Journal of the Brazilian Chemical Society 21 (2010) 2184–2188.

[29] A.P.C. Teixeira, B.R.S. Lemos, L.A. Magalhaes, J.D. Ardisson, R.M. Lago, C.A. Furtado, A.P. Santos, Journal of Nanoscience and Nanotechnology 12 (2012) 2661–2667.

[30] J.-P. Tessonnier, D.S. Su, ChemSusChem 4 (2011) 824–847.

[31] A. Thayer, Chemical and Engineering News 84 (2006) 29–30.

[32] D.E. Resasco, Large-scale Production and Commercialization of Single-walled Carbon Nanotubes of Controlled (n,m) Structure, American Chemical Society, 2004, pp. PRES-014.

[33] S. Crossley, J. Faria, M. Shen, D.E. Resasco, Science 327 (2010) 68–72.

[34] S. Drexler, J. Faria, M.P. Ruiz, J.H. Harwell, D.E. Resasco, Energy and Fuels 26 (2012) 2231–2241.

[35] P.A. Zapata, J. Faria, R.M. Pilar, D.E. Resasco, Topics in Catalysis 55 (2012) 38–52.

[36] L.C.A. Oliveira, M. Gonçalves, M.C. Guerreiro, T.C. Ramalho, J.D. Fabris, M.C. Pereira, K. Sapag, Applied Catalysis A: General 316 (2007) 117–124.

[37] F.C.C. Moura, M.H. Araujo, R.C.C. Costa, J.D. Fabris, J.D. Ardisson, W.A.A. Macedo, R.M. Lago, Chemosphere 60 (2005) 1118–1123.

[38] A.L. de Abreu, I.R. Guimarães, A.d.S. Anastácio, M.C. Guerreiro, Journal of Molecular Catalysis A: Chemical 356 (2012) 128–136.

[39] W.F. Souza, I.R. Guimaraes, D.Q. Lima, C.L.T. Silva, L.C.A. Oliveira, Energy and Fuels 23 (2009) 4426–4430.

[40] L. da Silva Madeira, V.S. Ferreira-Leitão, E.P. da Silva Bon, Chemosphere 71 (2008) 189–194.